Counterion-mediated, non-pairwise-additive attractions in bundles of like-charged rods

B.-Y. Ha and Andrea J. Liu
Department of Chemistry and Biochemistry, University of California at Los Angeles, Los Angeles, California 90095
(Received 18 February 1999)

Stiff polyelectrolyte chains, such as DNA, can attract each other in solution even though they have the same sign of charge. The attractions are mediated by multivalent counterions, which lead to an effective interaction at the two-chain level that is attractive at short range and repulsive at long range. However, the effective interchain interactions are not pairwise additive. We present a formulation that allows theoretical treatment of the many-chain problem without assuming pairwise additivity. We show that a bundle of chains held together by counterion-mediated attractions can be described in terms of a bulk and surface free energy, and discuss the temperature dependence of the attraction. [S1063-651X(99)00907-1]

PACS number(s): 87.14.Gg, 87.15.−v, 61.20.Qg, 61.25.Hq

I. INTRODUCTION

Experiments on solutions of stiff polyelectrolyte chains, such as DNA [1] or F-actin [2], clearly show that the like-charged chains can attract each other in the presence of multivalent ions of the opposite sign (counterions). Even long, stiff, charged viruses such as the tobacco mosaic virus and fd virus, which can be regarded as thick, stiff polyelectrolytes, exhibit attractions [2]. The fact that the attractions are observed for a wide range of stiff polyelectrolytes and a variety of multivalent counterions indicates that specific interactions are not responsible. Rather, there appears to be a general electrostatic mechanism that depends primarily on the valency of the counterion.

Another striking experimental feature is that the attractions do not appear to lead to macroscopic phase separation. Instead, the chains tend to form dense bundles of a fairly well-defined thickness [1,2]. Thus, the counterion-mediated interaction between the chains appears to have a different character from ordinary attractions that lead simply to phase separation at sufficiently high concentrations.

In addition to integral equation methods [3], two theoretical approaches have been used to explain the attractions. The first approach [4–7] was originally proposed by Oosawa [4] nearly thirty years ago, and is based on a charge fluctuation picture. In this picture, nonuniformities in the density of condensed counterions (i.e., counterions near the chains) along the chain length give rise to nonuniformities in the charge distribution that can become correlated from one chain to another, leading to a van der Waals-like attraction. This attraction increases with decreasing temperature, because the interchain charge correlations increase as the electrostatic interchain interaction increases relative to the thermal energy [5]. The valence of the counterion is important because the attraction between chains must be strong enough to overcome the repulsion due to the net charge on each chain. As the counterion valency increases, the attraction grows and the repulsion shrinks [6]. The second approach [8–11], originally proposed by Rouzina and Bloomfield [9], is based on a zero-temperature picture. At zero temperature, a system of chains and counterions should form a perfect, neutral ionic crystal, and it is not surprising that the interactions between chains are effectively attractive. The maximum depth of attraction decreases as the temperature increases and the ionic crystal melts [8]. A closely-related zero-temperature picture was recently proposed by Leikin and Kornyshev [12]. They suggest that the helical structure of DNA and the preference for specific binding sites on the DNA chain, rather than the condensed counterion interactions, determine the periodic structure for ions at zero-temperature that gives rise to an attraction.

Recently, we showed that the charge-fluctuation and ionic-crystal pictures are not contradictory, but actually are complementary to each other [13]. When we incorporated the nonzero ionic radius into the charge fluctuation approach, we found oscillatory charge correlations that grow in range as the temperature is lowered, and eventually diverge at the spinodal for the ionic crystal. Thus, at higher temperatures where the charge correlations are liquidlike, a charge fluctuation picture might more accurately describe the origin of the attraction, but at lower temperatures where the charge correlations are solidlike, the ionic crystal is a better description. We note that molecular dynamics simulations by Stevens [14] show that counterions diffuse quite rapidly and freely within the bundles, and are therefore not frozen in a crystalline arrangement.

In previous papers, we have shown that our results are in quantitative agreement with simulations [8] of the interaction between two infinite rods [6], but that the form of the two-rod interaction is not particularly useful because the effective interactions among rods are not pairwise-additive [7]. This is because the charge distributions on the rods can be affected by the presence of another rod. By calculating the free energy of an N-rod bundle explicitly, we showed that the breakdown of pairwise additivity leads to qualitative changes in the behavior of bundles. The assumption of pairwise additivity leads to the prediction that the equilibrium bundle size is finite, but the explicit calculation shows that the equilibrium bundle size is infinite. This appears to contradict the experimental observation of a well-defined finite bundle size. However, numerical simulations by Stevens [14] and a recent theoretical argument [15] suggest that the kinetics of bundle formation might set the bundle size, so that the system never reaches equilibrium.

The primary purpose of this paper is to provide a detailed description of our theoretical approach. Our model and the

calculations that lead to a closed form expression of the free energy of a bundle of N rods are presented in Sec. II. For small N, the free energy can be evaluated numerically by diagonalizing $N\times N$-dimensional matrices [7]. In the large N limit, it is possible to analyze the free energy analytically [16]. We have shown that in the salt-free case, it is possible to describe the free energy of a large bundle in terms of a bulk free energy and surface free energy [16]. In Sec. III, we extend the asymptotic analysis to the case of added salt. In Sec. IV, we address the controversial question of the temperature-dependence of the attraction. In Ref. [13], we showed that it is necessary to incorporate the nonzero radius of the ions in order to capture the correct temperature dependence of the charge correlations. Here, we show that the ionic size is also crucial to the temperature dependence of the inter-rod attractions. Once the ionic size is taken into account, we find that the depth of attraction increases as temperature decreases, in agreement with simulations [8]. Sec. V examines the dependence of our results on the lattice structure within the bundle. Finally, Sec. VI summarizes the advantages and disadvantages of our approach.

II. MODEL AND FREE ENERGY

A. Model

In our calculations, we study a bundle of N negatively-charged rods parallel to the z-direction and placed on a lattice in the xy-plane. Inside a condensed DNA bundle, the concentration is very high, with a center-to-center chain spacing of 25 Å (DNA itself has a diameter of roughly 20 Å); at comparable bulk concentrations, DNA packs in a hexagonal lattice [17]. Our analytical expressions are completely general and apply to any lattice structure, but we have typically assumed a square lattice for our numerical calculations. We will discuss the dependence on lattice structure in Sec. V.

Each rod consists of M monomers of length b, and each monomer carries a negative charge of $-f_0$ (in units of the electronic charge e) that is assumed to be distributed uniformly. Note that the actual charge distribution for DNA is helical; this nonuniform distribution can also lead to attractions at very short distances and low temperatures [12], but we have not adopted this more realistic description here. The positively charged counterions have radius r_c and charge Z. In reality, the counterions are distributed with some spatial density profile around the rods, which can be approximated by the solution to the nonlinear Poisson-Boltzmann equation. We adopt the two-state approximation to describe this density distribution; that is, we divide the counterions into two classes, condensed and free [4,18]. A condensed counterion is approximated to lie on the nearest monomer, and to add a charge Z to the net charge of that monomer, while a free counterion contributes to Debye screening of the electrostatic interactions in the solution. Note that recent calculations by Kardar and Golestanian [19] avoid the two-state assumption by expanding around the Poisson-Boltzmann result. Their calculation provides some justification for the two-state model: when they approximate the counterion distribution with a step function, they recover our results. Expanding around the Poisson-Boltzmann solution with its spatial distribution of counterions (without assuming a step function) is a definite improvement over our theory, but this approach is quite complicated to apply to our bundle system, and it also assumes point ions. Although our two-state approach is crude, it does allow us to include the nonzero ionic radius, as we have done in Sec. IV.

We define f_c to be the average number of condensed counterions per monomer; we do not assume that f_c is determined by the Manning criterion, but solve for it self-consistently as a function of the number of rods and the lattice constant a. Because condensed counterions can move along the rods or exchange with free counterions, the effective charge of a monomer can fluctuate. The charge on monomer s of rod j can assume the values

$$q_j(s) = -f_0 + mZ, \tag{1}$$

where $m=0,1,2,3$, etc. is the number of condensed counterions occupying a given monomer. If we assume that a large number of condensed counterions can be assigned to a given monomer, then we can apply the central limit theorem to the charge distribution, and can treat the charge per monomer, $q_j(s)$ as a Gaussian variable. Thus, we characterize the charge distribution by two quantities: the net charge on the rod and the variance in the charge of a monomer on the rod, given, respectively, by

$$q \equiv \langle q_j(s)\rangle_q, \quad \delta q^2 \equiv \langle (q(s)-\langle q_i(s)\rangle)^2\rangle_q = Z^2 f_c, \tag{2}$$

where the average $\langle \ldots \rangle_q$ is over all realizations of charge distribution. Note that identical expressions for q and δq^2 in terms of f_c and Z have been derived by an independent method by Golestanian [20].

In the absence of interactions, charges at different sites are assumed to be uncorrelated:

$$\langle \delta q_i(s)\, \delta q_j(s')\rangle_q = \delta_{ij}\delta(s-s'). \tag{3}$$

In addition to the charges on the rods, there are mobile ions in solution (free counterions and salt ions). We allow for these by including free ions labeled by the index α, carrying charge q_α. For simplicity, we assume that the counterions are identical to one of the ionic species of the added salt, although the theory can easily be extended to the more general case. We also assume that the concentration of rods is very low, so that the concentration of free ions is negligible compared to the concentration of salt ions (this is true under experimental conditions [1,2]). In this case, the mobile ions can be treated as overall neutral [21]. Finally, it is useful to introduce the Bjerrum length, $\ell_B = e^2/\epsilon k_B T$, namely the length scale at which the electrostatic energy is comparable to the thermal energy $k_B T$. We will also use the dimensionless Bjerrum length in units of the monomer length, $\tilde{\ell}_B \equiv \ell_B/b$. The Manning-Oosawa parameter [4,18], a measure of the ratio of the electrostatic energy to the thermal energy, is given by $\xi = \tilde{\ell}_B f_0$ in our notation.

In terms of the charge variables $q_j(s)$ on the rods and the mobile ions q_α, along with their associated positions $\mathbf{r}_j(s)$ and $\mathbf{r}_\alpha$, the electrostatic interaction Hamiltonian is

$$\beta\mathcal{H}=\frac{1}{2}\ell_B\left[\sum_{ij}^{N}\sum_{ss'}^{M}\frac{q_i(s)q_j(s')}{|\mathbf{r}_i(s)-\mathbf{r}_j(s')|}+2\sum_{i}^{N}\sum_{s}^{M}\sum_{\alpha}\frac{q_i(s)q_\alpha}{|\mathbf{r}_i(s)-\mathbf{r}_\alpha|}+\sum_{\alpha\alpha'}\frac{q_\alpha q_{\alpha'}}{|\mathbf{r}_\alpha-\mathbf{r}_{\alpha'}|}\right]. \quad (4)$$

Charge neutrality requires $\Sigma_j\Sigma_s q_j(s)+\Sigma_\alpha q_\alpha=0$.

B. Derivation of free energy

The system can adjust the monomer charges $q_i(s)$ but not their positions $\mathbf{r}_i(s)$. It can also adjust the free ion positions $\mathbf{r}_\alpha$, but not their charges q_α. The partition function is therefore the sum over all realizations of the charge variables $q_i(s)$ and the functional integral over the free ion positions $\mathbf{r}_\alpha$:

$$\mathcal{Z}=\int\mathcal{D}\mathbf{r}_\alpha\langle e^{-\beta\mathcal{H}}\rangle_q=\int\mathcal{D}\mathbf{r}_\alpha\int\mathcal{D}q_i(s)e^{-\beta\mathcal{H}}, \quad (5)$$

where the electrostatic Hamiltonian is given by Eq. (4). To see the effect of mobile ions on the interaction between two charges on the rods, we integrate over positions of mobile ions first. In order to treat the two-body $q_\alpha q_\beta$ interactions, we use the Hubbard-Stratanovich transformation to replace the two-body interactions with a one-body interaction of the charge with an effective dimensionless electrostatic potential $\Psi(\mathbf{r})$:

$$\mathcal{Z}=\int\mathcal{D}\mathbf{r}_\alpha\left\langle\left\langle\exp\left\{-\frac{1}{2}\ell_B\left[\sum_{ij}^{N}\sum_{ss'}^{M}\frac{q_i(s)q_j(s')}{|\mathbf{r}_i(s)-\mathbf{r}_j(s')|}+2\sum_{i}^{N}\sum_{s}^{M}\sum_{\alpha}\frac{q_i(s)q_\alpha}{|\mathbf{r}_i(s)-\mathbf{r}_\alpha|}+i\sum_{\alpha}q_\alpha\Psi(\mathbf{r}_\alpha)\right]\right\}\right\rangle_q\right\rangle_\Psi. \quad (6)$$

Here, the average over realizations of Ψ, $\langle\cdots\rangle_\Psi$ is with respect to the probability distribution

$$\mathcal{W}_\Psi=\exp\left[-\frac{1}{2}\int\int d\mathbf{r}d\mathbf{r}'\Psi(\mathbf{r})v^{-1}(\mathbf{r},\mathbf{r}')\Psi(\mathbf{r}')\right], \quad (7)$$

where $v^{-1}(\mathbf{r},\mathbf{r}')$ is the inverse of $\beta v(\mathbf{r},\mathbf{r}')=\ell_B/|\mathbf{r}-\mathbf{r}'|$.

Equation (6) is exact, and for point charges q_α, the averages can be carried out exactly. However, we assume that fluctuations in the density of mobile ions are small, and retain only terms in Eq. (6) up to order Ψ^2. We make this approximation in order to treat the mobile charges and the fixed charges on the rods in a consistent way.

Up to $O(\Psi^2)$, the partition function is then given by

$$\mathcal{Z}\propto\exp\left[-\frac{1}{2}\mathrm{tr}\ln(1+\beta n_s v)-\frac{1}{2}\beta\,\mathrm{tr}(n_s\overline{v})\right]\times\int\mathcal{D}q_j(s)\int\mathcal{D}\mathbf{r}_\alpha\times\exp\left[-\frac{1}{2}\beta\sum_{ij}\sum_{ss'}q_i(s)q_j(s')\overline{v}(\mathbf{r}_i(s)-\mathbf{r}_j(s'))\right]. \quad (8)$$

Here, we have used the matrix

$$n_s(\mathbf{r},\mathbf{r}')=n_s\delta(\mathbf{r}-\mathbf{r}'), \quad (9)$$

where n_s is the number density of mobile ions. In addition, we have introduced the effective interaction $\overline{v}$, defined by

$$\overline{v}(\mathbf{r},\mathbf{r}')=[v^{-1}+n_s]^{-1}(\mathbf{r},\mathbf{r}'). \quad (10)$$

This effective interaction is simply the screened Coulomb interaction, given in Fourier space by

$$\beta\overline{v}(\mathbf{q})=\frac{4\pi\ell_B}{\mathbf{q}^2+\kappa_s^2}, \quad (11)$$

where $\kappa_s^2=8\pi\ell_B I$, where I is the ionic strength of the solution. Thus, tracing over the mobile ion positions at Gaussian order is equivalent to Debye-Hückel theory [5]. The Gaussian approximation is valid when $\epsilon k_B T>Z^2e^2n_s^{1/3}$ (in the case of a Z:Z salt) [22].

The next step is to average over all possible charge distributions on the rods [the average over $q_j(s)$]. Note that we still have a two-body screened Coulomb interaction $q_i(s)q_j(s')$. We again use the Hubbard-Stratanovich transformation to replace this two-body interaction with a one-body interaction of the charge with an effective dimensionless electrostatic potential $\Phi(\mathbf{r})$:

$$\mathcal{Z}=\left\langle\left\langle\exp\left[-i\sum_{j=1}^{N}\sum_{s=1}^{M}q_j(s)\Phi(\mathbf{r}_j(s))\right]\right\rangle_q\right\rangle_\Phi, \quad (12)$$

where the average over realizations of Φ, $\langle\cdots\rangle_\Phi$, is with respect to the probability distribution

$$\mathcal{W}_\Phi=\exp\left[-\frac{1}{2}\int\int d\mathbf{r}d\mathbf{r}'\Phi(\mathbf{r})\overline{v}^{-1}(\mathbf{r},\mathbf{r}')\Phi(\mathbf{r}')\right], \quad (13)$$

where $\overline{v}^{-1}(\mathbf{r},\mathbf{r}')$ is the inverse of $\beta\overline{v}(\mathbf{r},\mathbf{r}')=\ell_B\exp[-\kappa_s|\mathbf{r}-\mathbf{r}'|]/|\mathbf{r}-\mathbf{r}'|$. The averages over $q_j(s)$ and $\Phi(\mathbf{r})$ cannot be evaluated exactly so we again retain only terms in Eq. (12) up to order Φ^2. This amounts to keeping two-point correlations in the condensed counterions by taking Gaussian fluctuations in $q_j(s)$ [6], and is valid when the charge fluctuations along the rods are not strong. Just as the Gaussian approximation for Ψ led to Debye-Hückel theory for the mobile ions, the Gaussian approximation for Φ leads to a one-dimensional Debye-Hückel theory for the monomeric charges. However, it is not a standard one-dimensional theory because the monomeric charges interact with each other, and with the charges on other rods, via three-dimensional screened interactions $\overline{v}$. In other words, our approximation is equivalent to treating each rod as a one-dimensional Debye-Hückel system that interacts with itself and with all the other rods via a three-dimensional Debye-Hückel system of mobile ions.

Because of the geometry of the many-rod system, which is nonuniform with the rods in specified positions, the computation of the interaction between rods is nontrivial, even up to order Φ^2. We first integrate over Φ to obtain a compact expression for the rod-rod interaction:

$$\beta\mathcal{F}_{\rm bundle}=\frac{1}{2}q^2\mathscr{V}_B\sum_{ij}\sum_{ss'}[\delta_{ij}-(1+\beta\delta q^2\bar{v})^{-1}_{is,js'}]\frac{1}{\delta q^2}+\frac{1}{2}\mathrm{tr}\ln[1+\beta\delta q^2\bar{v}]-(\text{self-energy}), \tag{14}$$

where the trace ''tr'' is over all rods and monomers. If the rods are not parallel or if N is finite, the free energy in Eq. (14) cannot be diagonalized, and the free energy must be computed numerically.

The following discussion of how to further simplify Eq. (14) applies only when the rods are parallel and infinitely long. In that case, we can use translational invariance along the rod axes to write the matrix element $(\bar{v})_{is,js'}$ as $(\bar{v})_{is,js'}=(\bar{v})_{i,j;|s'-s|}$. The free energy $\mathcal{F}_{\rm bundle}$ can then be partially diagonalized by introducing a Fourier transform in the z-direction (along the rod axes). For example, note that the trace that appears in Eq. (14) can be written out as

$$\frac{1}{2}\mathrm{tr}\ln[1+\beta\delta q^2\bar{v}]=\sum_{is}\sum_{\ell=0}^{\infty}\frac{(-1)^{\ell+1}}{\ell}(\beta\delta q^2)^l(\bar{v}^{\ell})_{is,is}. \tag{15}$$

We now Fourier transform from s to k_z and replace the convolution integral with a product of the Fourier transformed matrix elements:

$$\sum_{s}\sum_{s_1}\cdots\sum_{s_{\ell-1}}\beta^{\ell}\bar{v}_{is,i_1s_1}\cdots\bar{v}_{i_{\ell-1}s_{\ell-1},is}=L\int_{-\infty}^{\infty}\frac{dk_z}{2\pi}\beta^l\underbrace{\bar{v}_{i,i_1}(k_z)\cdots\bar{v}_{i_{\ell-1},i}(k_z)}_{\ell\ \text{powers}} \tag{16}$$

where $\beta\bar{v}_{ij}(k_z)=2\mathscr{V}_BK_0(R_{ij}\sqrt{\kappa_s^2+k_z^2})$, with R_{ij} the distance between rods i and j and $R_{ii}\equiv b$. We then have

$$\tfrac{1}{2}\mathrm{tr}\ln\left[1+\beta\delta q^2\bar{v}\right]=\frac{L}{2}\int_{-\infty}^{\infty}\frac{dk_z}{2\pi}\sum_{\ell=0}^{\infty}\sum_{i}\cdots\sum_{i_{\ell-1}}\frac{(-1)^{\ell+1}}{\ell}\delta q^2\underbrace{\bar{v}_{i,i_1}(k_z)\cdots\bar{v}_{i_{\ell-1},i}(k_z)}_{\ell\ \text{powers}}. \tag{17}$$

Similarly, the inverse matrix that appears in Eq. (14) is

$$\sum_{ij}\sum_{ss'}(1+\beta\delta q^2\bar{v})^{-1}_{is,js'}=\sum_{i}\cdots\sum_{i_{\ell}}\sum_{s}\cdots\sum_{s_{\ell}}\sum_{\ell=0}(-1)^{\ell}\times(\beta\delta q^2)^{\ell}\bar{v}_{is,i_1s_1}\cdots\bar{v}_{i_{\ell-1}s_{\ell-1},js'}. \tag{18}$$

If we have translational invariance, then the summation over $\{s\}$ can easily be performed; in terms of ${}^0\bar{v}_{ij}\equiv\bar{v}_{ij}(k_z=0)$, we have

$$\sum_{s}\cdots\sum_{s'}\bar{v}_{is,i_1s_1}\cdots\bar{v}_{i_{\ell-1}s_{\ell-1},js'}=L\,{}^0\bar{v}_{i,i_1}\cdots{}^0\bar{v}_{i_{\ell-1},j}. \tag{19}$$

Both terms in Eqs. (16) and (19) can be resummed. If we define matrices $M(k)$ and ${}^0M$ to be

$${}^0M_{ij}=\delta q^{-2}\delta_{ij}+2\mathscr{V}_BK_0(\kappa_sR_{ij}),$$

$$M_{ij}(k_z)=\delta q^{-2}\delta_{ij}+2\mathscr{V}_BK_0(R_{ij}\sqrt{\kappa_s^2+k_z^2}), \tag{20}$$

then the electrostatic free energy per monomer of the rods, for $a\ll L$, is

$$\beta\mathcal{F}_{\rm bundle}(a)=\frac{1}{2}q^2\sum_{ij}\left[\delta_{ij}-\frac{1}{\delta q^2}{}^0M^{-1}_{ij}\right]\frac{1}{\delta q^2}+\frac{b}{2}\int_{-\infty}^{\infty}\frac{dk_z}{2\pi}\ln[\det\delta q^2M(k_z)]-bN\delta q^2\mathscr{V}_B\times\int_{-\infty}^{\infty}\frac{dk_z}{2\pi}K_0(b\sqrt{\kappa_s^2+k_z^2}), \tag{21}$$

where $K_0(x)$ is the zeroth-order modified Bessel function of the second kind.

The first term in Eq. (21) represents the effective repulsion among the rods, which is screened due to the condensed counterions and mobile ions. The second term represents the attraction due to fluctuations in the monomeric charge. When $N=2$, then the free energy in Eq. (21) reduces to that for two rods [see Eq. (6) in Ref. [6]]. The last term is the self-energy that must be subtracted from the free energy. Note that the free energy in Eq. (21) cannot be written as the pairwise sum of the two-rod interaction. The electrostatic free energy can only be given as a sum of pair interactions when we retain only the leading term in the expansion of Eq. (21) in powers of δq^2 (i.e., up to monopole-dipole interactions). Podgornik and Parsegian [23] also concluded that pairwise additivity is invalid, based on an analysis that includes up to dipole-dipole interactions [up to the second term in the expansion of Eq. (21)]; in contrast, our technique includes all higher multipole interactions, which are required because the multipole expansion diverges at low temperature or short rod separations.

The electrostatic free energy in Eq. (21) depends on the average number of condensed counterions per monomer, f_c. We could simply use the Manning criterion [18] to set f_c. However, that criterion applies only to a single, infinitely long rod, and the proximity of other rods should enhance counterion condensation. We therefore solve for f_c self-consistently. We enclose the bundle in a large cylinder of radius $L_\perp$ and length L, and construct the total free energy in terms of the number of condensed and free counterions. We then equate the chemical potentials of condensed and free counterions. The total free energy valid for $\kappa_s^{-1} \ll L$ is then

$$\beta\mathcal{F}_{\text{total}} = Nf_c\left(\ln\frac{f_c M v_0}{Lb^2} - 1\right) + \left(Nf_f + \frac{1}{2}n_s b L_\perp^2\right) \times\left[\ln\left(\frac{Nf_f M}{LL_\perp^2} + \frac{n_s}{2}\right)v_0 - 1\right] + \frac{1}{2}nbL_\perp^2(\ln nv_0/2 - 1) - NZq\tilde{\ell}_B f_f K_0(\kappa_s b) + \beta\mathcal{F}_{\text{bundle}} - \frac{LL_\perp^2}{12\pi}\kappa_s^3, \tag{22}$$

where $f_f = (f_0 - Zf_c)/Z$ is the number of free counterions per monomer and $v_0 = 4/3\pi r_c^3$ is the counterion volume. The first three terms in Eq. (22) correspond to the entropy of mixing; the first describes the entropy of condensed counterions confined to a volume which is smaller than the total available space by a factor of $b^2/L_\perp^2$, the second term corresponds to the mobile cations and the third term corresponds to mobile anions. The last term is the standard Debye-Hückel result for the salt ions.

The fourth term in Eq. (22) deserves some detailed discussion. It is the contribution to the electrostatic free energy from condensed counterions and rods given in Eq. (21). This term is needed to set the reference potential for free counterions; if the interaction between a rod and a free counterion is set to zero when they are separated by a distance much larger than κ_s^{-1}, then this term is the decrease in free energy due to condensation. Since we enforce condensation from the beginning instead of charging the rods with counterions [see Eq. (4)], this term does not naturally arise from our previous calculations. When an infinitesimal charge $\delta q'$ (per monomer) is added to a negatively charged rod of net charge q', the change in the electrostatic energy of the rod is

$$\beta\delta E = -N\tilde{\ell}_B q' dq' \int_{-\infty}^{\infty} dz \frac{e^{-\kappa_s z}}{z}. \tag{23}$$

This charging process continues until the rod has net charge of q. Thus the free energy we need is an integration of Eq. (23) over q' from 0 to q multiplied by the number of rods N. This leads to the fourth term in Eq. (22).

C. ''Fermion'' version of model

The model introduced in the previous section assumes that an indefinitely large number of counterions can be assigned to a given monomer. One can also consider a variant of this model [24,11], where each rod consists of M sites, and each site can either be empty or occupied by one counterion. In this case, the charge fluctuation is no longer given by Eq. (2) but is given by

$$\delta q^2 = Z^2 f_c - Z^2 f_c^2. \tag{24}$$

Obviously, the expression for the average charge remains unchanged; $q = -f_0 + Zf_c$. The corresponding entropic free energy of condensed counterions per site can be obtained by setting v_0/ab^2 to unity:

$$\beta\mathcal{F}_{\text{ent. cond}} = f_c(\ln f_c - 1). \tag{25}$$

The difference in the entropy of condensed counterions is negligible, because the total entropy is dominated by the free counterions. Thus, both models predict essentially the same values for f_c. The difference between the ''fermion'' model and the previous ''boson'' model therefore lies only in the different expressions for δq^2. Note that the ''fermion'' model predicts a weaker attraction because δq^2 is smaller in this case. In particular, the ''fermion'' model predicts no attraction at $T=0$ for monovalent counterions because there is complete condensation ($f_c = 1$, or $\delta q^2 = 0$), whereas the ''boson'' version yields an attraction that saturates in that limit.

III. ASYMPTOTIC ANALYSIS OF THE FREE ENERGY

In the previous section, we derived a closed-form expression for the free energy of a bundle of a fixed number of rods, N. In the asymptotic limit $N \to \infty$, it turns out that the free energy in Eq. (21) can be further simplified analytically, when the rods are parallel and infinitely long. In this section, we will show that the free energy per rod becomes N-independent for $N \gg 1$. In other words, the free energy $\mathcal{F}_{\text{bundle}}$ is extensive. The asymptotic analysis will justify our finding in Ref. [7] that the equilibrium bundle size is either $N=1$ or $N=\infty$, and that the free energy $\mathcal{F}_{\text{bundle}}$ changes monotonically with N.

At first glance, it is surprising that $\mathcal{F}_{\text{bundle}}$ is extensive, especially when there is no added salt to screen the Coulomb interactions, since the system carries finite net charge Q that grows linearly with N, i.e., $Q = Nq$. If we calculate the free energy by summing over all pairs of rods using the effective two-rod interaction, then we would obtain a repulsive interaction of a bundle which increases like N^ν with $\nu > 1$. Thus, the assumption of pairwise additivity leads to a superextensive free energy. However, we showed by explicit calculation of Eq. (21) in Ref. [16] that in the case of no added salt, it is possible to describe a large bundle in terms of a bulk free energy F_{bulk} and a surface free energy F_{surface}. In other words, the bundle free energy for $N \gg 1$ can be written as $\mathcal{F}_{\text{bundle}} \sim NF_{\text{bulk}} + \sqrt{N}F_{\text{surface}}$, where F_{bulk} and F_{surface} are independent of N. Here we will extend the analysis presented in Ref. [16] to the case of added salt.

Instead of taking the limit $N \to \infty$ directly to obtain the bulk free energy per rod, F_{bulk}, we will define a second system: an infinite lattice of rods made by replicating the N-rod bundle periodically, so that the $(N+1)$th rod has the same charge distribution as the first one. This system will have a free energy per bundle given by $\mathcal{F}_{\text{periodic}}$, which can

be written as in Eq. (21) in terms of two new matrices ${}^0\mathcal{M}$ and $\mathcal{M}(k_z)$:

$$
\begin{aligned}
{}^0\mathcal{M} &= \delta q^{-2}\delta_{\mathbf{j}_\perp \mathbf{j}'_\perp} + 2\tilde{\mathscr{V}}_B \sum_{k_x k_y} K_0(\kappa_s, k_z=0, \mathbf{k}_\perp) \\
&\quad \times \exp[-i\mathbf{k}_\perp \cdot \mathbf{j}_\perp], \\
\mathcal{M}(k_z) &= \delta q^{-2}\delta_{\mathbf{j}_\perp \mathbf{j}'_\perp} + 2\tilde{\mathscr{V}}_B \sum_{k_x k_y} K_0(\kappa_s, k_z, \mathbf{k}_\perp) \\
&\quad \times \exp[-i\mathbf{k}_\perp \cdot \mathbf{j}_\perp].
\end{aligned} \tag{26}
$$

Here, the matrix index $\mathbf{j}_\perp$ is conjugate to the rod positions on the lattice and assumes the values: $\mathbf{j}_\perp = (j_x, j_y)$, where $j_x, j_y = 0,1,\ldots,\sqrt{N}-1$. Upon substitution of Eq. (26) into Eq. (21), we obtain

$$
\begin{aligned}
\beta\mathcal{F}_{\text{periodic}} &= \frac{\tilde{\mathscr{V}}_B q^2}{{}^0K_0^{-1}(\kappa_s) + 2\tilde{\mathscr{V}}_B \delta q^2} + \frac{b}{2}\left(\frac{1}{N}\sum_{\mathbf{k}_\perp}\right) \\
&\quad \times \int_{-\infty}^{\infty} \frac{dk_z}{2\pi} \ln[1 + 2\tilde{\mathscr{V}}_B \delta q^2 K_0(\kappa_s, k_z, \mathbf{k}_\perp)] \\
&\quad - bN\delta q^2 \tilde{\mathscr{V}}_B \int_{-\infty}^{\infty} \frac{dk_z}{2\pi} K_0(b\sqrt{\kappa_s^2 + k_z^2}),
\end{aligned} \tag{27}
$$

where $\mathbf{k}_\perp$ is the wave vector conjugate to the periodically repeated bundle: $\mathbf{k}_\perp$ assumes the discrete values $\mathbf{k}_\perp = (2\pi/\sqrt{N})(n_x, n_y)$ where $n_x, n_y = 0,1,\ldots,\sqrt{N}-1$. The discrete Fourier transform of the modified Bessel function $K_0(R_{ij}\sqrt{\kappa_s^2 + k_z^2})$ is given by

$$
K_0(\kappa_s, k_z, \mathbf{k}_\perp) = \sum_{j_x j_y}^{\sqrt{N}-1} K_0(a|\mathbf{j}_\perp|\sqrt{\kappa_s^2 + k_z^2}) \exp[i\mathbf{k}_\perp \cdot \mathbf{j}_\perp]. \tag{28}
$$

The function ${}^0K_0(\kappa_s)$ that appears in the first term of Eq. (27) is simply ${}^0K_0(k_z = \mathbf{k}_\perp = 0)$.

The bulk free energy can now be obtained by taking the limit of $\mathcal{F}_{\text{periodic}}$ as $N \to \infty$. To take this limit, first note that $K_0(x) \sim (1/\sqrt{x})e^{-x}$ for $x \gg 1$, so that the sum $K_0(\kappa_s, k, \mathbf{k}_\perp)$ and ${}^0K_0(\kappa_s)$ both approach finite values, $\mathcal{K}_0(\kappa_s, k, \mathbf{k}_\perp)$ and ${}^0\mathcal{K}_0(\kappa_s)$, respectively, as $N \to \infty$. Furthermore, $\mathbf{k}_\perp$ becomes a continuous variable in the limit $N \to \infty$, so we can replace the sum $(1/N)\Sigma_{\mathbf{k}_\perp}$ by an integral $\int_0^{2\pi/a}[d\mathbf{k}_\perp/(2\pi)^2][\ldots]$ up to a correction of order $1/N$. The resulting bulk free energy per rod is then given by

$$
\begin{aligned}
\beta F_{\text{bulk}} &= \frac{\tilde{\mathscr{V}}_B q^2}{{}^0\mathcal{K}_0^{-1}(\kappa_s) + 2\tilde{\mathscr{V}}_B \delta q^2} \\
&\quad + \frac{b}{2}\int_0^{2\pi/a} \frac{d\mathbf{k}_\perp}{(2\pi)^2} \int_{-\infty}^{\infty} \frac{dk_z}{2\pi} \ln[1 \\
&\quad + 2\tilde{\mathscr{V}}_B \delta q^2 \mathcal{K}_0(\kappa_s, k_z, \mathbf{k}_\perp)] - b\,\delta q^2 \tilde{\mathscr{V}}_B \\
&\quad \times \int_{-\infty}^{\infty} \frac{dk_z}{2\pi} K_0(b\sqrt{\kappa_s^2 + k_z^2}).
\end{aligned} \tag{29}
$$

Thus, the free energy per rod approaches a constant, i.e., the bulk free energy F_{bulk}, in the limit of $N \to \infty$, in accord with our previous numerical results [7]. In other words, the free energy of a lattice of rods is extensive.

The next step is to look at a very large but finite bundle and to include the contribution of the bundle surface to the free energy. Note that we have considered a square lattice of rods, so there are $4\sqrt{N}$ rods at the surface of a square bundle of dimensions $\sqrt{N} \times \sqrt{N}$. To study the surface tension, we should consider the free energy difference

$$
4\sqrt{N}F_{\text{surface}} = \mathcal{F}_{\text{bundle}} - NF_{\text{bulk}}, \tag{30}
$$

and show that F_{surface} is independent of N in the limit $N \to \infty$. Here, $\mathcal{F}_{\text{bundle}}$ is given by Eq. (21) and is specified by the two matrices ${}^0M$ and $M(k_z)$ defined in Eqs. (20).

Let us first consider the difference between the free energy of the finite bundle and the free energy per bundle for the periodically-replicated bundle:

$$
\begin{aligned}
4\sqrt{N}\beta F_{\text{diff}} &= \beta\mathcal{F}_{\text{bundle}} - \beta\mathcal{F}_{\text{periodic}} \\
&= \frac{1}{2}\sum_{ij} [({}^0\mathcal{M}^{-1}\,{}^0\mathcal{M}\,{}^0\mathcal{M}^{-1})_{ij} \\
&\quad - ({}^0\mathcal{M}^{-1}\,{}^0M\,{}^0\mathcal{M}^{-1})_{ij}] \frac{q^2}{\delta q^4} \\
&\quad + \frac{b}{2}\int_{-\infty}^{\infty} \frac{dk}{2\pi} \ln\det[1 + \mathcal{M}^{-1}(k) \cdot (M(k) \\
&\quad - \mathcal{M}(k))].
\end{aligned} \tag{31}
$$

Now note that in the limit of an infinite bundle, $N \to \infty$, we must recover ${}^0M \to {}^0\mathcal{M}$ and $M(k) \to \mathcal{M}(k)$. This enables us to expand F_{diff} in powers of ${}^0\mathcal{M}^{-1} \cdot ({}^0M - {}^0\mathcal{M})$ and $\mathcal{M}^{-1}(k)[M(k) - \mathcal{M}(k)]$ for large N. After subtracting the self-energy, we find

$$
\begin{aligned}
\beta F_{\text{diff}} &= -\frac{1}{4}\tilde{\mathscr{V}}_B q^2 \left(\frac{1}{1 + 2\tilde{\mathscr{V}}_B \delta q^2\, {}^0K_0(\kappa_s)}\right)^2 \\
&\quad \times \left| \frac{\mathbf{k}_\perp}{k_\perp} \cdot \boldsymbol{\nabla}_{\mathbf{k}_\perp} K_0(\kappa_s, \mathbf{k}_\perp) \right|_{\mathbf{k}_\perp = 0} \\
&\quad + \frac{b}{2}\left| \left(\frac{1}{N}\right) \sum_{\mathbf{k}_\perp} \int_{-\infty}^{\infty} \frac{dk_z}{2\pi} K_0(\kappa_s, k_z, \mathbf{k}_\perp) \right. \\
&\quad \left. \times \frac{\mathbf{k}_\perp}{k_\perp} \cdot \boldsymbol{\nabla}_{\mathbf{k}_\perp} \left[\frac{\tilde{\mathscr{V}}_B^2 \delta q^4 K_0(\kappa_s, k_z, \mathbf{k}_\perp)}{1 + 2\tilde{\mathscr{V}}_B \delta q^2 K_0(\kappa_s, k_z, \mathbf{k}_\perp)} \right] \right|.
\end{aligned} \tag{32}
$$

This is a generalization of our earlier result [see Eq. (12) in Ref. [16]] to the case of added salt. Again, we can replace $(1/N)\Sigma_{\mathbf{k}_\perp}[\ldots]$ by $\int_0^{2\pi/a}[d\mathbf{k}_\perp/(2\pi)^3]$, up to a correction of order $1/N$. We then find that

$$
F_{\text{diff}} \to \text{const} \times (1 + O(1/N)) \tag{33}
$$

in the limit $N \to \infty$.

The quantity $F_{\rm diff}$ is related to the desired surface tension $F_{\rm surface}$ by the equation

$$4\sqrt{N}F_{\rm surface}=4\sqrt{N}F_{\rm diff}+\mathcal{F}_{\rm periodic}-NF_{\rm bulk}. \quad (34)$$

However, by comparing Eq. (27) to Eq. (29), we see that the leading correction to $\mathcal{F}_{\rm periodic}-NF_{\rm bulk}$ comes from replacing the sum over discrete values of $\mathbf{k}_\perp$ by an integral. This correction is of order $1/N$. Therefore,

$$\mathcal{F}_{\rm periodic}=NF_{\rm bulk}(1+O(1/N)). \quad (35)$$

Given Eqs. (34) and (35), we find that $F_{\rm surface}$ approaches an N-independent constant as $N\to\infty$, with corrections of order $1/\sqrt{N}$.

In the no-salt limit, $\kappa_s\to 0$, we have shown in Ref. [16] that the surface free energy originates only from the attractive interactions characterized by the charge fluctuations δq^2. This follows from the fact that ${}^0K_0(\kappa_s)\sim N$ in that limit and thus the first term in Eq. (32) vanishes like $1/N^2$.

In summary, we can combine Eqs. (29) and (32) to write the bundle free energy $\mathcal{F}_{\rm bundle}$ as

$$\mathcal{F}_{\rm bundle}\cong NF_{\rm periodic}+4\sqrt{N}\mathcal{F}_{\rm diff}\cong NF_{\rm bulk}+4\sqrt{N}F_{\rm surface}+O(1), \quad (36)$$

where $F_{\rm bulk}$ and $F_{\rm surface}$ are independent of N. Thus, a large bundle can be described as the sum of a bulk free energy and a surface free energy. This result is useful to phenomenological theories of bundle nucleation, etc. Why does the long-ranged repulsion between rods not lead to super-extensive scaling of the free energy? The reason lies in the breakdown of pairwise-additivity of the effective rod-rod interactions. The long-ranged repulsion between rods is highly screened in the explicit calculation because charge fluctuations are correlated over many rods, not just pair by pair. This results in an extensive bundle free energy, in accord with rigorous arguments on electrostatic systems [25].

A. Limiting behavior of surface free energy

To test our result for the surface free energy, let us take the limiting case of vanishing lattice constant, $a\to 0$, such that $\delta q^2/a^2b=Z^2n$ remains constant, where n is the number density of condensed counterions. This corresponds to taking the continuum limit of the lattice of rods. In this limit, the system reduces to a Debye-Hückel electrolyte. Then we have $2\delta q^2\tilde{\ell}_B K_0(\kappa_s,k_z,\mathbf{k}_\perp)=4\pi\tilde{\ell}_B/(a^2\mathbf{k}_\perp^2+a^2\kappa_s^2+b^2k_z^2)$. If we use this expression in Eq. (32), then we obtain

$$\beta F_{\rm surface}\sim\left(\frac{a}{b}\right)\times\begin{cases}\delta q^2\tilde{\ell}_B & \text{if } \kappa_s^2a^2\ll\delta q^2\tilde{\ell}_B\\ \delta q^4\tilde{\ell}_B^2/\kappa_s^2a^2 & \text{if } \kappa_s^2a^2\gg\delta q^2\tilde{\ell}_B.\end{cases} \quad (37)$$

In the low salt limit, as $\kappa_s\to 0$, the surface free energy per unit area, i.e., the surface tension, varies as $(a/b)\delta q^2\tilde{\ell}_B\sim\kappa_c^2$, where κ_c^{-1} is the Debye screening length associated with condensed counterions. This agrees with an earlier result of Onsager [26], which was obtained by solving the linearized Poisson-Boltzmann equation for a Debye-Hückel electrolyte in contact with an immiscible medium. In order to calculate the surface tension, Onsager introduced a spatially varying screening length $\kappa(\mathbf{r})$. Solving the linearized Poisson-Boltzmann equation with a spatially varying $\kappa(\mathbf{r})$ was quite difficult. The alternate approach that we have presented here is a systematic treatment of the surface tension using functional integral methods, and is equivalent to solving the linearized Poisson-Boltzmann equation with a step function approximation to the ion density. The main advantage of our approach is that it can easily be applied to more general systems such as our bundle of rods.

In the low salt limit, Eq. (37) shows that the surface free energy is independent of salt concentration and increases linearly with the Bjerrum length. On the other hand, in the high salt limit, the surface free energy decreases with increasing salt concentration, and becomes negligible when $\kappa_s^2a^2\gg\delta q^2\tilde{\ell}_B$. These results make physical sense. Surface effects arise because the charge fluctuations along the rods suddenly decay to zero at the outer surface of the bundle. This gives rise to a dipole layer at the outer boundary. In the low salt case, this dipole layer cannot polarize the surrounding solution, so the surface energy (in units of the thermal energy) increases linearly with the strength of the electrostatic interactions (the Bjerrum length). In the high salt case, on the other hand, the system can lower its free energy by forming an induced dipole layer across the boundary. In other words, the charge fluctuations along the rods at the surface of the bundle tend to polarize the surrounding ionic solution; this polarized solution then interacts with the charges on the rods. This is a *second* order effect, so it results in a second order dependence of the surface free energy on the amplitude of the charge fluctuations: $\beta F_{\rm surface}\propto\delta q^4\tilde{\ell}_B^2$. Finally, in the extreme high salt limit $\kappa_s^2a^2\gg\delta q^2\tilde{\ell}_B$, the rods are so highly screened that they no longer interact with each other, and there is no difference between a rod at the surface and a rod deep within the bundle. In that case, the surface free energy of the bundle vanishes. The condition $\kappa_s^2a^2\gg\delta q^2\tilde{\ell}_B$ is equivalent to the condition $\kappa_s\gg\kappa_c$, where κ_c^{-1} is the screening length due to condensed counterions: $\kappa_c^2=4\pi\delta q^2\ell_B/a^2b$. In other words, if the screening due to salt overwhelms the screening due to condensed counterions on the rods, then the surface free energy is negligible.

B. When are the interactions pairwise-additive?

From our analysis of the surface free energy, it is clear that many-body effects are unimportant when the salt concentration is high enough. This is because the salt screens the correlations between charges over many rods that are responsible for the breakdown of pairwise additivity [23]. Thus, we should recover pairwise additivity at high ionic strength. On the other hand, if there are no charge fluctuations along the rods, $\delta q^2=0$, then the interaction between rods is purely repulsive and pairwise additivity should again be valid. Therefore the criterion for pairwise additivity should depend on both κ_s and δq^2. In fact, we find that pairwise additivity is valid when

$$\delta q^2\tilde{\ell}_B\ll\kappa_s^2a^2. \quad (38)$$

Under these conditions, the expansion of the attractive part of the free energy in powers of $\delta q^2\tilde{\ell}_B$ is convergent [i.e., the

multipole expansion is convergent; see Eq. (21)]. Note that under the conditions of Eq. (38), the surface free energy is negligible [see Eq. (37)]. This is not surprising; when the interactions are so highly screened that inter-rod charge correlations can be neglected, then pairwise additivity is recovered and there is no difference between surface rods and rods deep inside the bundle.

We note that the criterion Eq. (38) always corresponds to the regime where the interactions between rods are repulsive. For the case $\kappa_s = 0.1$ Å^{-1}, pairwise additivity is valid when $a \gg 30$ Å. When $\kappa_s = 0.001$ Å^{-1}, pairwise additivity is valid when $a \gg 3000$ Å. In both cases, the interactions between rods are repulsive and extremely weak in this regime. Thus, whenever the counterion-mediated interactions are *attractive*, pairwise additivity is not valid.

Recently, Shklovskii argued that the validity of pairwise additivity should also depend on the rod radius. His arguments are based on the ionic crystal picture of a salt-free solution, where the counterions form a Wigner crystal in a background provided by the charged rods [10]. He distinguishes between two regimes characterized by the dimensionless parameter Zb/r_{rod}, where r_{rod} is the rod radius. He argues that the interaction is not pairwise-additive if $Zb/r_{\mathrm{rod}} \gg 1$. In the regime where $Zb/r_{\mathrm{rod}} \ll 1$, on the other hand, he argues that the counterion-mediated interaction is pairwise-additive because the rod radius is sufficiently large compared to the lattice spacing that only nearest-neighbor rods interact via their facing surfaces, which are almost planar. It is not straightforward to compare our criterion to his, since we assume infinitely thin rods and he assumes no added salt. In order to compare our results, we now modify our criterion to include the nonzero rod radius. Note that for fixed temperature, counterion valence and linear charge separation b, the charge fluctuations per monomer remain fixed as the rod radius increases. However, the surface area of the monomer increases, so the charge fluctuation/surface area decreases. This leads to a decrease in the effective value of δq^2. As a result, the regime over which the rod-rod interaction is pairwise-additive increases as r_{rod} increases. Using this argument, our criterion for pairwise-additivity can be generalized to

$$\delta q^2 \ell_B \ll \left(\frac{a^2}{L^2}\right)\left(\frac{r_{\mathrm{rod}}}{b}\right), \quad \kappa \to 0. \tag{39}$$

For finite δq^2, this inequality can be met only when the radius of rods is much larger than the length of rods. Our criterion is therefore much more stringent than Shklovskii's and depends on the length of the rods as well as on their radius.

Why is our criterion so different from Shklovskii's? Shklovskii assumes that as long as two rods of nonzero radius are sufficiently close so that their facing surfaces are nearly planar, then the interaction can be described as a pairwise sum of attractions described by correlated charge distributions on two-dimensional surfaces (the two-surface calculation has been carried out by Rouzina and Bloomfield [9]). It is not clear that this guarantees pairwise-additivity of rod-rod interactions, however. Consider three rods, A, B, and C, in a triangular arrangement. Rods A and B, B and C, and C and A all interact along their facing surfaces. Shklovskii assumes that the AB, BC, and CA interactions are pairwise additive. However, the charge distribution on the surface of rod A that interacts with rod B could be correlated with the charge distribution on the surface of rod A that interacts with rod C. This correlation would lead to a breakdown of pairwise-additivity. This could be the origin of the discrepancy between our criterion and Shklovskii's.

IV. TEMPERATURE DEPENDENCE OF ATTRACTION

In all of our earlier calculations, we fixed the temperature and studied the dependence of counterion-mediated interactions on the lattice spacing, screening length, counterion valency, and other parameters. Here, we focus on the temperature dependence, which has been controversial in the literature. In the discussion that follows, we will imagine that we can vary temperature without varying the dielectric constant. In reality, the dielectric constant tends to vary as $1/T$, so that the Bjerrum length, $\ell_B = e^2/\epsilon k_B T$ is roughly constant. For our purposes, however, we will assume that lowering T is equivalent to raising the Bjerrum length.

Brownian dynamics simulations by Grønbech-Jensen and coworkers [8] show unambiguously that the counterion-mediated attraction between two rods is strongest at zero temperature, and weakens with increasing temperature. This is in accord with the picture proposed by Rouzina and Bloomfield [9], where the attraction originates from the fact that the system forms an ionic crystal at zero temperature. Thus, the counterions form an ordered array between the two rods that brings them together at low temperatures.

At higher temperatures, however, this ionic crystal melts and the distribution of counterions along the rods is more liquidlike than solidlike. At these temperatures, one can develop a complementary picture, where nonuniformities of the charge distribution along the rods become correlated from one rod to another, and lead to attractions. It has often been argued that this picture, since it is based on thermal fluctuations of the charge distribution, should lead to an attraction that *increases* with increasing temperature, in contradiction with the simulations. In fact, this was the conclusion of Oosawa [4], who first proposed the picture. This argument is erroneous, however. The temperature dependence is more complex because the attraction also relies on *correlations* between the charge distributions on the two rods; electrostatic interactions between the rods give rise to the correlation, whereas thermal fluctuations tend to decrease the correlation. Barrat and Joanny [5] introduced a perturbation expansion in powers of $\delta q^2 \ell_B$ and showed that to second order, the inter-rod correlation leads to an attraction that actually increases with decreasing temperature. Another factor that works in this direction is the effect of temperature on counterion condensation. As the temperature decreases, the amount of counterion condensation increases, so the net charge q per monomer decreases. As a result, the repulsion between the rods decreases, giving an effective attraction that increases with decreasing temperature.

Someone familiar with Debye-Hückel theory, which is also based on a charge fluctuation picture, might consider the temperature dependence to be trivial. In an electrolyte solution, the Debye-Hückel limiting law yields a free energy that varies as $-\sqrt{\ell_B} \sim -1/\sqrt{T}$. Thus, Debye-Hückel theory yields

an attraction that increases with decreasing temperature. One might therefore expect that our calculation, where we consider one-dimensional Debye-Hückel systems interacting with themselves and with each other via three-dimensional Debye-Hückel interactions, to yield a similar result. It turns out, however, that the situation in our rod system is not quite so simple. Note that the form of Eq. (6) in Ref. [6] leads to an attraction that *vanishes* at $T=0$. The exact solution of a similar model, on the other hand, leads to an attraction that is strongest at $T=0$ [11]. We find that the origin of the discrepancy lies in our assumption that the ion radius is zero. In our system, charges on different rods are discrete because the rods are placed at discrete lattice points. It turns out to be important to treat intra-rod charge correlations at the same level, so that charges on the same rod are also discrete.

In an earlier paper [13], we showed that we can capture the correct temperature behavior of the charge correlation function if we incorporate the nonzero radius of the ions along the rods. The most straightforward way to include the ionic radius along the rods is to allow short-ranged charge correlations over the ionic size. We introduce the one-dimensional structure factor for a segment of length D [13]: $g(s-s')=\Theta(|s-s'|-D)/D$. Given this structure factor, we found that the charge correlations along the axis of a given rod are oscillatory with an exponential decay. As the temperature is lowered, the exponential decay length increases, so that the correlations become longer-ranged. Finally, at a very low temperature, the decay length diverges. This signals the spinodal to the ionic crystal; this is where the high-temperature ''liquidlike'' phase becomes unstable to an ionic crystal. Thus, we were able to show that our approach is fully compatible with the low temperature picture proposed by Rouzina and Bloomfield and others [9,8,10].

Here, we extend the analysis in Ref. [13] to the free energy. When we include the nonzero ionic size, the attractive term in the free energy [the second term in Eq. (14)] becomes

$$\frac{1}{2}\mathrm{tr}\ln[1+\beta\delta q^2\bar{v}]\rightarrow\frac{1}{2}\mathrm{tr}\ln[1+\beta\delta q^2 g\bar{v}]$$
$$=\sum_{is}\sum_{\ell=0}^{\infty}\frac{(-1)^{\ell+1}}{\ell}(\beta\delta q^2)^{\ell}((\bar{v}g)^{\ell})_{is,is}, \tag{40}$$

where g is a matrix defined by $g_{is,js'}=\delta_{ij}\Theta(|s'-s|-D)/D$. Here, $\Theta(x)$ is the step function. In the case of parallel, infinitely long rods, we can Fourier transform in the z direction as before, and we find that the free energy of a bundle is still given by Eq. (21) except that the matrix $M(k)$ is now given by

$$\delta q^2 M_{ij}(k_z)\rightarrow\delta_{ij}+2\tilde{\ell}_B\delta q^2 g(k_z)K_0(R_{ij}\sqrt{\kappa_s^2+k_z^2}), \tag{41}$$

where $g(k_z)=\sin k_z D/k_z D$ is the Fourier transform of $\Theta(|s'-s|-D)/D$. Note that the repulsive part of the free energy, namely the first term in Eq. (21), is unaffected by the inclusion of the nonzero ion radius. This is because the repulsive term is governed by the zero-k_z component of $M_{ij}(k_z)$, and $g(k_z=0)\equiv 1$.

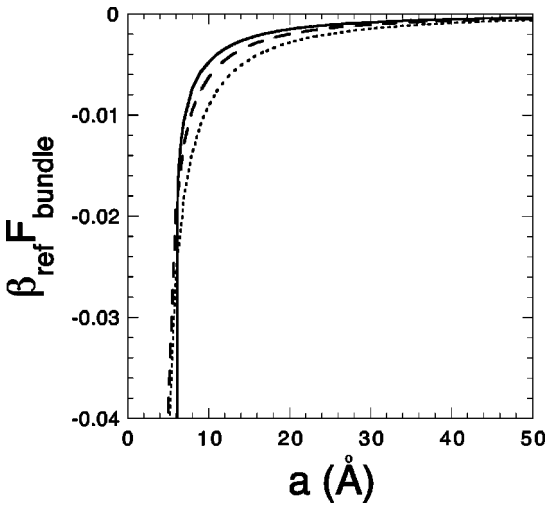

FIG. 1. Temperature dependence of the attraction (low salt). We have plotted the free energy per monomer per rod, F_{bundle}, as a function of a, for a 16-rod bundle on a square lattice at low salt, $\kappa=0.001$ Å^{-1}. The reference temperature is room temperature (300 K). There are three curves corresponding to different temperatures: $\ell_B=6$ Å (solid), $\ell_B=9$ Å (dashed), and $\ell_B=12$ Å (dotted). Note that the attraction is strongest at small lattice spacings a for the largest value of ℓ_B (the lowest temperature). However, the trend reverses at higher values of a; this is an artifact of the way in which we introduce the nonzero ion radius.

We now use Eq. (41) to compute the bundle free energy as a function of temperature, or equivalently, of the Bjerrum length ℓ_B. In Figs. 1 and 2, we have plotted the free energy of a 16-rod bundle as a function of the lattice spacing a for

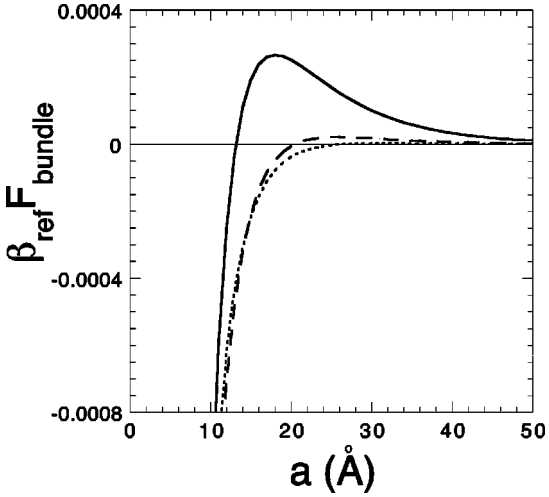

FIG. 2. Temperature dependence of the attraction (high salt). We have plotted the free energy per monomer per rod, F_{bundle}, as a function of a, for a 16-rod bundle on a square lattice at high salt, $\kappa=0.1$ Å^{-1}. The reference temperature is room temperature. As in Fig. 1, there are three curves corresponding to different temperatures: $\ell_B=6$ Å (solid), $\ell_B=9$ Å (dashed), and $\ell_B=12$ Å (dotted). The main effect of lowering temperature is to increase the amount of counterion condensation; this lowers the repulsive barrier.

three different values of ℓ_B. Our parameters are $b = 1.7$ Å, $M = 10^5$, $Z = 2$, and $D = 4.2$ Å. The free energy is plotted in units of the thermal energy at room temperature ($T = 300$ K). First consider the behavior at low salt ($\kappa = 0.001$ Å^{-1}) described by Fig. 1. We find that the interaction between rods becomes more attractive as ℓ_B increases (T decreases), for small values of the lattice constant a. However, the attraction is weaker as ℓ_B increases when a is large. This is probably an artifact of our approximation for the nonzero ion size, as we discuss further below. Note that our curves look different from the simulation results [8] because we have not included a short-ranged excluded volume repulsion between the rods and counterions. As a result, the free energy becomes increasingly attractive as a decreases, instead of reaching a minimum and becoming repulsive at very small a. Because of this, we cannot extract the free energy at the minimum. Nevertheless, the fact that the attraction grows as ℓ_B increases for small a suggests that the minimum is deeper at high ℓ_B, or equivalently, low T, in agreement with the simulations.

At high salt concentrations ($\kappa_s = 0.1$ Å^{-1}), Fig. 2 shows that the system develops a significant barrier in the free energy [7]. As ℓ_B is increased, the barrier is lowered and the attraction increases. This is again consistent with the low temperature ionic crystal picture. Note that the repulsive barrier decreases with increasing ℓ_B mainly because the amount of counterion condensation increases, and the net charge therefore decreases.

We now turn to the potentially disturbing result that the attraction appears to weaken with decreasing T at large lattice spacing a of the bundle. Is it possible that the origin of this unphysical result is the Gaussian approximation (random phase approximation)? We believe that the problem lies in the way in which we have included the nonzero ionic size through a one-dimensional form factor. Instead of doing a perturbative calculation, we could carry out a self-consistent calculation for the charge structure. The net result would be to replace the one-dimensional form factor $g(s)$ with the charge correlation function, which would be solved for self-consistently. Such an approach would lead to a more accurate description of the system. However, it would not affect our most important result, which is that the equilibrium bundle size is infinite [7]. This is because the attraction will still be short-ranged, while the repulsion will be unaffected by the form of $g(s)$ because $g(k_z = 0)$ is still unity. The requirement that $g(k_z = 0) = 1$ is known for electrolyte solutions as the Stillinger-Lovett second moment condition [27].

V. DEPENDENCE ON LATTICE STRUCTURE

In all of the calculations so far, we assumed that the rods in the bundle were organized into a square lattice. This is an unphysical choice of lattice structure; the true structure is hexagonal [17]. It is important to note that our model is unphysical in that condensed counterions are placed directly on the rod, leading to charge fluctuations along the rod. In a hexagonal packing, the anticorrelation between charges on neighboring rods leads to frustration. In reality, the counterions sit in between the rods, so there is no frustration when the rods are hexagonally packed. The advantage of a square lattice is that it avoids the unphysical consequences of frustration incurred by the hexagonal lattice within our model. It is, however, worthwhile to compare the free energy of a square-lattice bundle with that of a hexagonal-lattice bundle. This comparison is shown in Fig. 3 (the thin solid curves marked with squares represent results for the square lattice, while the thick solid lines represent results for the hexagonal lattice). Note that free energy is somewhat lower for the hexagonal lattice, showing that the hexagonal lattice is more stable even though there is frustration. We have plotted the screened repulsive and attractive contributions separately dashed and dotted curves, respectively) to show that while the repulsion is slightly stronger for the hexagonal lattice, as expected, the attraction is significantly stronger also, leading to a lower free energy for the hexagonal case. It is not too surprising that frustration does not prevent the hexagonal lattice from being more stable, since we are not at extremely low temperatures. For our parameters, the ordering of the counterions along the rods is liquidlike, not solidlike, and the anticorrelation in charge from one rod to the next is not too large, so the effects of frustration are relatively weak.

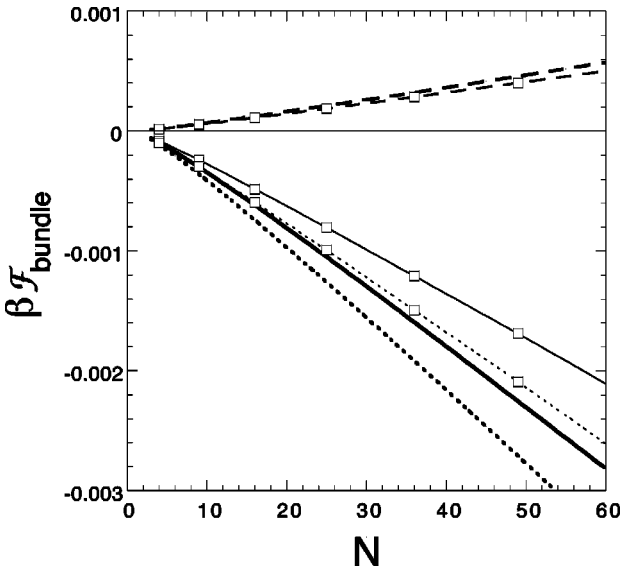

FIG. 3. Dependence on lattice structure. We have plotted the free energy of a bundle, $\mathcal{F}_{\text{bundle}}$, as a function of the number of rods N in the bundle, for two different lattice structures: hexagonal (thick curves) and square (thin curves with squares). The lattice constant is $a = 30$ Å, the salt concentration is $\kappa_s = 0.07$ Å^{-1}, and the Bjerrum length is 7.1 Å. The solid lines correspond to the total free energy $\mathcal{F}_{\text{bundle}}$. We have also plotted the attractive and repulsive contributions separately, as the dotted and dashed curves, respectively. Note that the magnitude of the repulsion is very similar for both lattice structures, but the attractive contribution is larger for the hexagonal lattice. This is what makes the hexagonal lattice more stable.

VI. SUMMARY

The general approach that we have adopted, of describing the rods with associated condensed counterions as one-dimensional Debye-Hückel systems coupled to each other through a three-dimensional Debye-Hückel ionic solution, relies on the first term in a perturbation (loop) expansion that probably diverges in the regime of interest. However, good approximations can be useful beyond their range of validity.

The important question is: what physics is left out by our description? In the case of *simple* Debye-Hückel theory, two important qualitative effects are left out: ionic associations (counterion condensation) and the possibility of oscillatory charge correlations. We have gone beyond the simple theory by including counterion condensation within a two-state model. We have also shown that it is important to include the nonzero ionic radius, so that the charge distribution along the rod is discrete, not continuous. This leads to qualitatively correct behavior in the charge correlations [13], which are oscillatory with an exponential decay length that increases with decreasing temperature, as well as the correct temperature trend at small separations of the rods. Thus, although our approximations will not lead to *quantitatively* accurate behavior at low temperatures, they predict the correct *qualitative* behavior.

Since our approach predicts a transition to an ionic crystal at low temperatures, it bridges the gap between the ''charge fluctuation'' picture and the zero temperature ''ionic crystal'' picture. However, this is mainly a conceptual advantage: our approach is not the best one at extremely low temperatures, because the model itself is not accurate there. The condensed counterions sit *on* the rods in our model, whereas they really should sit in between the rods. In other words, the structure of the ionic crystal is not captured correctly by the model. This is probably a source of greater quantitative error at low temperatures than is the Gaussian approximation.

The main advantage of the formulation presented here is that it leads to a tractable analysis of the many-rod problem. This is especially important because many-rod interactions lead to qualitatively different behavior than is predicted by the pairwise sum of two-rod interactions [7]. Moreover, it shows that for large bundles, the simple approach of treating the bundle free energy as the sum of a bulk free energy and a surface free energy is valid. This is important to phenomenological treatments of bundles. Finally, our formulation can be used to study questions relevant to kinetics, such as the energetic factors that govern the kinetics of bundle formation [15].

ACKNOWLEDGMENTS

We gratefully acknowledge the support of the National Science Foundation through Grant No. DMR-9619277.

[1] V.A. Bloomfield, Biopolymers **31**, 1471 (1991); V.A. Bloomfield, Curr. Opin. Struct. Biol. **6**, 334 (1996), and references therein.
[2] J.X. Tang, S. Wong, P. Tran, and P. Janmey, Ber. Bunsenges. Phys. Chem. **100**, 1 (1996); J.X. Tang, T. Ito, T. Tao, P. Traub, and P.A. Janmey, Biochemistry **36**, 12 600 (1997), and references therein.
[3] S. Marcelja, Biophys. J. **61**, 1117 (1992).
[4] F. Oosawa, Biopolymers **6**, 134 (1968); Polyelectrolytes (Marcel Dekker, New York, 1971).
[5] J.L. Barrat and J.F. Joanny, Adv. Chem. Phys. **94**, 1 (1996).
[6] B.-Y. Ha and A.J. Liu, Phys. Rev. Lett. **79**, 1289 (1997).
[7] B.-Y. Ha and A.J. Liu, Phys. Rev. Lett. **81**, 1011 (1998).
[8] N. Grønbech-Jensen, R.J. Mashl, R.F. Bruinsma, and W.M. Gelbart, Phys. Rev. Lett. **78**, 2477 (1997).
[9] I. Rouzina and V.A. Bloomfield, J. Phys. Chem. **100**, 9977 (1996).
[10] B. Shklovskii, Phys. Rev. Lett. (to be published).
[11] J. J. Arenzon, J. F. Stilck, and Y. Levin, e-print cond-mat/9806358.
[12] A.A. Korynshev and S. Leikin, J. Chem. Phys. **107**, 3656 (1997); Biophys. J. **75**, 2513 (1998).
[13] B.-Y. Ha and A.J. Liu, Phys. Rev. E **58**, 6281 (1998).
[14] M.J. Stevens, Phys. Rev. Lett. **82**, 101 (1999).
[15] B.-Y. Ha and A.J. Liu, Europhys. Lett. (to be published).
[16] B.-Y. Ha and A.J. Liu, Physica A **253**, 235 (1998).
[17] D. Durand, J. Doucet, and F. Livolant, J. Phys. II **2**, 1769 (1992).
[18] G.S. Manning, J. Chem. Phys. **51**, 954 (1969).
[19] M. Kardar and R. Golestanian, Rev. Mod. Phys. (to be published).
[20] R. Golestanian (unpublished).
[21] S. A. Safran, *Statistical Thermodynamics of Surfaces, Interfaces and Membranes* (Addison-Wesley, Reading, MA, 1994).
[22] P. M. Chaikin and T. C. Lubensky, *Principles of Condensed Matter Physics* (Cambridge University Press, Cambridge, England, 1995), pp. 204–208.
[23] R. Podgornik and V.A. Parsegian, Phys. Rev. Lett. **80**, 1560 (1998).
[24] M. Olvera de la Cruz, L. Belloni, M. Delsanti, J.P. Dalbeiz, O. Spalla, and M. Drifford, J. Chem. Phys. **103**, 5781 (1995).
[25] E.H. Lieb, Rev. Mod. Phys. **48**, 553 (1976).
[26] L. Onsager and N.N. Nicholas, J. Chem. Phys. **2**, 258 (1934).
[27] F.H. Stillinger and R. Lovett, J. Chem. Phys. **48**, 3858 (1968).